Influence of the Oxygen Substoichiometry and of the Hydrogen Incorporation on the Electronic Band Structure of Amorphous Tungsten Oxide Films

ARTICLE *in* THE JOURNAL OF PHYSICAL CHEMISTRY C · JUNE 2014

Impact Factor: 4.77 · DOI: 10.1021/jp502092h

THE JOURNAL OF PHYSICAL CHEMISTRY C

Article

pubs.acs.org/JPCC

Influence of the Oxygen Substoichiometry and of the Hydrogen Incorporation on the Electronic Band Structure of Amorphous Tungsten Oxide Films

Maria Vasilopoulou,[†] Ioannis Kostis,[†,‡] Nikolaos Vourdas,[†] Giorgos Papadimitropoulos,[†] Antonios Douvas,[†] Nikolaos Boukos,[†] Stella Kennou,[‡] and Dimitris Davazoglou*[,†]

[†]Institute of Nanoscience and Nanotechnology, NCSR "Demokritos", 153 10 Agia Paraskevi, Attiki, Greece

[‡]Department of Electronics, Technological and Educational Institute of Pireus, 12244 Aegaleo, Greece

[§]Department of Chemical Engineering, University of Patras, 26500 Patras, Greece

Supporting Information

ABSTRACT: The influence of the oxygen substoichiometry and of the hydrogen incorporation on the electronic structure of amorphous tungsten oxide films was investigated. It was found that both of them cause the appearance of intermediate bands (IBs) within the energy gap; approximately 3 and 1 eV below the edge of the conduction band (CB), respectively. The hydrogen is incorporated into the W−O network bonding either to the oxygen or to the tungsten ions. In the former case, the electronic structure of the material retains the characteristics of amorphous stoichiometric tungsten oxide with, additionally, the two IBs. In the latter case, the electronic structure of tungsten oxide is seriously perturbed because in addition to the IBs the 1s orbitals of the hydrogen also contribute to the formation of the edges of valence and CBs causing the delocalization of electrons. Carriers donated by the incorporated hydrogen ions are excited in the CB, causing plasma oscillations and red shifting photoluminescence.

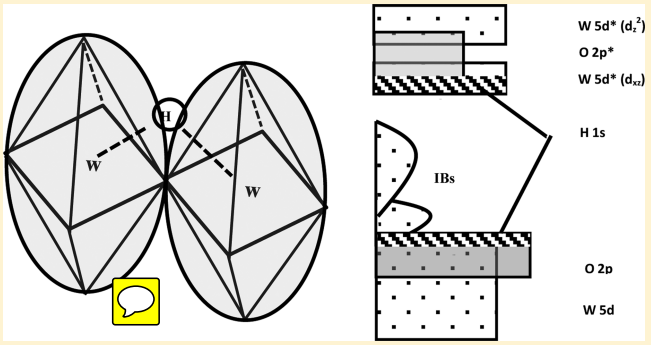

I. INTRODUCTION

Tungsten trioxide is a perovskite whose lattice is formed by WO_6 octahedra connected between them by sharing the corner oxygen ions, with channels formed between them.[1,2] Light ions, such as hydrogen and alkali metals, may be easily incorporated through these channels into the bulk or the surface of the material (reversibly under voltage application, change of chemical environment, temperature, etc.), and during this doping process, the basic W−O network remains intact. Doping induces serious alterations in the electronic structure of the material, which are reflected strikingly on its optical and electrical properties, which has led to applications of tungsten oxide in areas such as the electrochromic (EC),[3] and gasochromic (GC)[4] "smart" windows and the gas sensors.[5] So, while undoped tungsten oxide is transparent and insulating, exhibiting a band gap of 3 eV,[6] when lightly doped, it appears blue and exhibits electrical conductivity or even characteristics of a degenerated semiconductor such as gap narrowing and the appearance of free carriers in the conduction band (CB).[7] One additional factor causing alterations in the electronic structure of this oxide is the presence of oxygen vacancies (oxide substoichiometry), which also enhance the optical absorption (therefore causing coloration) and the electrical conductivity of the oxide.[8] Finally, the electronic structure of tungsten oxide is affected by the detailed arrangement of W and O ions in space, and this explains the variety of band gaps reported in literature.[6]

The optical and electrical properties in doped tungsten oxide were initially explained assuming the formation of tungsten bronzes[9] (M_xWO_3, where M is the intercalated metallic ion), whose electronic structure was considered to be similar to that of WO_3 with conduction electrons, however, present in the CB donated by the dopants (the so-called rigid band approximation[10]). The rigid band approximation was not verified experimentally[11−13] and insulator-to-metal transitions were observed for Na- and H-doped WO_3 at ratios of 0.25 and 0.32, respectively.[14−16] Other models were also proposed to explain the electrical and optical properties of doped tungsten oxide summarized in ref 17, but it is clear that more work is needed to understand the role of oxygen vacancies and the interaction of dopants with the host network.

The alterations in the electronic structure of tungsten bronzes and "colored" tungsten oxide films relatively to the corresponding "uncolored" WO_3 have been shown by X-ray and UV photoelectron spectroscopy (XPS and UPS, respectively),[8,18−20] and the most striking one is the appearance

Received: February 28, 2014
Revised: May 21, 2014

   dx.doi.org/10.1021/jp502092h | J. Phys. Chem. C XXXX, XXX, XXX−XXX

of intermediate bands (IBs) within the band gap, distant from the CB by 1 to 2 eV, indicating that electrons at the corresponding states are potentially related to the optical properties of the material within the visible and near-IR. The sensitivity of the electronic structure to factors such as the substoichiometry and the atomic arrangement was also demonstrated theoretically in a previous work,[21] where it was shown that intermediate states appear within the gap dependent on the distance between neighboring W−W ions and the corresponding oxygen bridging. Experimentally, except for the various gaps reported,[6] the sensitivity of the electronic structure was shown in a series of recent papers,[22−24] where by changing the deposition environment (oxidizing or reducing) and doping with atomic hydrogen we obtained tungsten oxide layers with properties corresponding to undoped[21] and to degenerated semiconductors[23] and semimetals at various degrees.[22,23] These layers were successfully used to modify electrodes in organic light-emitting diodes and solar cells to inject and extract carriers in hybrid organic−inorganic electronic devices through these intermediate gap states.[25−28]

We investigate the incorporation of hydrogen in amorphous tungsten oxide with various stoichiometries and its influence on the electronic structure of this material. The study is based on Fourier transform infrared (FTIR) spectroscopy, spectroscopic ellipsometry (SE), and photoluminescence spectroscopy (PS), combined with XPS and UPS. We show that, similarly to the case of amorphous MoO_3,[29] oxygen vacancies (substoichiometry) act as deep donors, while incorporated hydrogens act as shallow donors, giving rise to two IBs within the band gap. The incorporated hydrogen may be bonded either with the O forming OH^- ions connected between them by hydrogen bonds or with the W ions. In the former case, the material remains semiconductor with two IBs within the band gap, while in the latter, contrary to what was observed for MoO_3 films,[29] the electronic states at the edges of valence and conduction bands (VB and CB) delocalize. With further incorporation of hydrogen in the material, free electrons are thermally excited at the bottom of the CB and at even higher concentration of oxygen vacancies the band gap starts to decrease because valence and IBs start merging.

II. EXPERIMENTAL SECTION

A. Samples Preparation. Tungsten oxide films were deposited in a deposition system previously described[24,28] on Si pieces with dimensions of 2 × 2 cm^2 cut from (100) Si wafers. Before deposition, substrates were given a piranha clean,[30] washed in ultrapure water, and dried in a nitrogen stream. The system consisted of a stainless-steel reactor in which the sample was positioned on an aluminum susceptor, 2 cm below a tungsten filament heated by an (AC) current lead by two Cu leads. The filament temperature was controlled by the current using calibration data obtained with a tiny thermocouple mechanically fixed on it. All depositions in this work were made with a filament temperature of 660 °C, which results in amorphous films. Deposition time was used to control film thickness, and because times up to 60 s were used and because of the high thermal mass of the aluminum susceptor, the substrate temperature was remaining near room temperature during deposition. The base pressure used was 80 mTorr, which was set using a commercial pressure stabilization system containing a diaphragm pressure gauge (Baratron) and a PC-driven needle valve allowing for the flow of one of various gases such as O_2, N_2, forming gas (FG, a mixture 90% N_2−10% H_2), and H_2 through the reactor, thus setting the deposition environment. The system was also equipped with two atomic layer deposition (ALD) valves, turning on and off within 50 ms. In this work, H_2 was pulse-injected into the rector through an ALD valve from an orifice situated above the turned-on filament; the injection caused an increase in pressure to 1 Torr, and the duration of the pressure pulse was on the order of 1 s. Probably atomic hydrogen was produced during injection that doped the film. It is noted that the production of atomic hydrogen is expected at filament temperatures much higher than 660 °C. However, anticipated results reported next, the tungsten oxide films exposed to pulse injection of hydrogen differ substantially from those deposited with hydrogen present in the deposition ambient, indicating doping by atomic hydrogen. Moreover, the increase in the deposition pressure during injection (by more than an order of magnitude) decreases the free mean path of gases in the chamber, so probably the enhanced concentration of hydrogen atoms near the filament and, additionally, the local presence of oxygen atoms are possible to catalyze the formation of atomic hydrogen.

B. Characterization Techniques. The deposited tungsten oxide films were characterized with a variety of optical techniques including FTIR spectroscopy (in absorption mode) using a Brooker spectrometer with SE within the 350−1000 nm range using a J. A. Woolam M2000F rotating compensator ellipsometer (RCE) running the WVASE32 software at an angle of incidence of 75.14°. The dispersion of the refractive index of films was modeled using one, two, or, in some cases, three Lorentz oscillators while for films exposed to atomic hydrogen (see later) one Lorentz and one Drude oscillator were used. PL spectra were recorded with a Horiba Jobin-Yvon iHR320 spectrometer with a He−Cd laser (325 nm, 3.81 eV) as the excitation source. The spectrometer was calibrated with an accuracy of 0.06 nm using the 365.015 nm Hg line. To obtain mutually comparable PL spectra, we positioned samples at the laser beam with high accuracy using a holder specially designed for this purpose.

The X-ray photoelectron spectroscopy (XPS) measurements were made in a Leybold/Specs MAX 200 spectrometer under ultrahigh vacuum (UHV) (~10^{-10} Torr) equipped with a Leybold EA-11 analyzer and using the unmonochromatized Mg Kα line (with photon energy of 1253.6 eV) at 15 keV and 20 mA anode current. The instrument was calibrated for the Au 4f 7/2 peak giving a full width at half-maximum of 1.3 eV. The oxide stoichiometry was estimated using the XPS-measured W 4f and O 1s core-level spectra. To this end, after a Shirley background subtraction, the areas under the photoemission peaks were integrated by fitting the O 1s and W 4f spectra with asymmetric Gaussian−Lorentzian curves. The error is estimated at ±10% in all XPS-derived atomic percentages. The VB spectra of W oxides were evaluated after recording the ultraviolet photoemission (UPS) spectra of 10 nm thick films deposited on Si substrate. For the UPS measurements, the same spectrometer was used as that for the XPS measurements using now the HeI (21.22 eV) excitation line. The analyzer resolution was determined from the width of the Au Fermi edge to be 0.16 eV.

III. RESULTS AND DISCUSSION

As previously reported, the deposited tungsten oxide films were highly disordered-amorphous independent of the deposition environment.[22−24] (See also Figures S1 and S2 in the

dx.doi.org/10.1021/jp502092h | J. Phys. Chem. C XXXX, XXX, XXX−XXX

Supporting Information.) XPS analysis was performed to investigate the chemical composition of the outermost film layers. The W 4f photosignals of the XPS spectra of tungsten oxide samples grown in N_2 and FG environments without and with the simultaneous injection of H_2 pulses (to create atomic hydrogen during deposition) are presented in Figure 1.

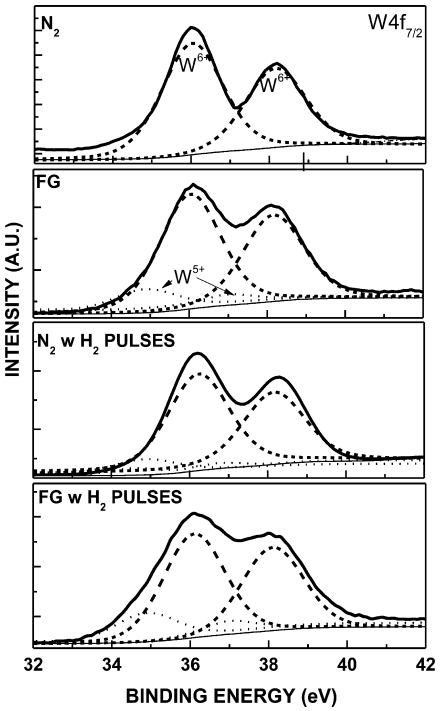

Figure 1. Surface W 4f XPS photoelectronic signals and their deconvolution taken on tungsten oxide samples grown in N_2 and FG environments without and with pulsed injection of hydrogen during deposition.

For the film deposited in the N_2 environment, the deconvolution of the W 4f photoemission peak was performed using two peaks with nearly equal width (fwhm = 1.7 eV) with the binding energy (BE) of W $4f_{7/2}$ centered at 36.0 ± 0.1 eV and that of W $4f_{5/2}$ at a BE of 38.2 ± 0.1 eV (with a peak ratio of 4:3). The position and the shape of these peaks are representative of W atoms with an oxidation state +6, as expected for stoichiometric WO_3.[31−33]

For films deposited in FG, the W 4f signal was broadened toward lower BEs, suggesting the presence of W oxidation states lower than +6. The deconvolution of the spectrum revealed the presence of two distinct doublets: the major components arising from W^{6+} and a second doublet at lower BEs (BE of (W $4f_{7/2}$) =34.8 eV and of (W $4f_{5/2}$) =37.1 eV with fwhm = 1.8 eV and a peak ratio 4:3), corresponding to 20.1% of the overall W atoms. This new doublet was attributed to the presence of W^{5+} ions, indicating that these films are substoichiometric (reduced),[34,35] with ∼20% of the tungsten atoms exhibiting a valence of +5.

Films deposited in N_2 and FG with injection of H_2 pulses were also found to be substoichiometric (reduced) with the contribution of peaks attributed to W^{5+} states in their XPS W 4f spectrum to be 7 and 25% of the total, respectively.

A similar analysis was done to O 1s peaks, as seen in Figure 2, where the deconvoluted XPS O 1s spectra of all samples are reported. For the sample deposited in N_2, the oxygen peak

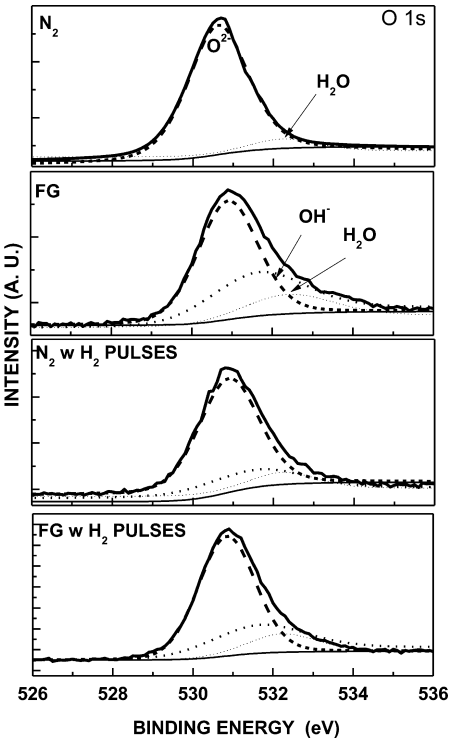

Figure 2. XPS spectra and deconvolution of the O 1s core levels taken on tungsten oxide samples grown under the same conditions as those in Figure 1.

(O^{2-}) located at ∼530.6 eV is observed together with a shoulder at 532.4 eV, which is attributed to adsorbed water vapor from the ambient air.[36] For the rest of samples, an additional contribution appears around 531.5 eV attributed to the presence of hydroxyl (OH^-). The film deposited in FG has the largest amount of OH^- groups (26% of the total oxygen species), while the injection of H_2 pulses during deposition induces a decrease in the concentration of these groups to 16.5 and 9.5% for films deposited in FG and N_2 environments, respectively. On the contrary, the contribution of the peak assigned to adsorbed water molecules is fairly the same in all samples, as expected, because they have been exposed to air before measurements.

From Figures 1 and 2, several conclusions may be drawn: Samples grown in N_2 environment are stoichiometric or very near stoichiometry. This is because the vapors formed at the filament are composed of clusters of (almost) stoichiometric tungsten oxide molecules.

In FG environment, the hydrogen atoms interact with the external oxygen atoms of the clusters and either stabilize forming hydroxyl radicals or form water, which is removed under vacuum, leaving behind an oxygen defective cluster. So, films grown in FG are substoichiometric and hydrogenated with the hydrogen atoms incorporated in the form of hydroxyl ions.

Surprisingly, films deposited in FG with simultaneous injection of H_2 pulses during growth exhibit lower hydrogen content than those without injection. A possible mechanism that can explain their composition is that the atomic hydrogen ions created during H_2 injection react with the hydroxyl ions of the clusters forming water molecules removed in the deposition ambient,[37] again creating substoichiometric vapors. However, this mechanism occurs only during the hydrogen pulse, that is,

dx.doi.org/10.1021/jp502092h | J. Phys. Chem. C XXXX, XXX, XXX−XXX

approximately 1 to 2 s, so during the rest of deposition time the deposit has a composition similar to that deposited in FG environment without the injection previously described, and this explains the appreciable OH^- content (16.5%) in these films.

Finally, samples grown in N_2 ambient with H_2 injection are oxygen-deficient and exhibit the lowest hydrogen content, and their composition may be explained by similar mechanisms as those occurring for samples grown in FG previously described.

f3 In Figure 3 are shown FTIR spectra taken on tungsten oxide samples deposited in N_2 and FG environments without and

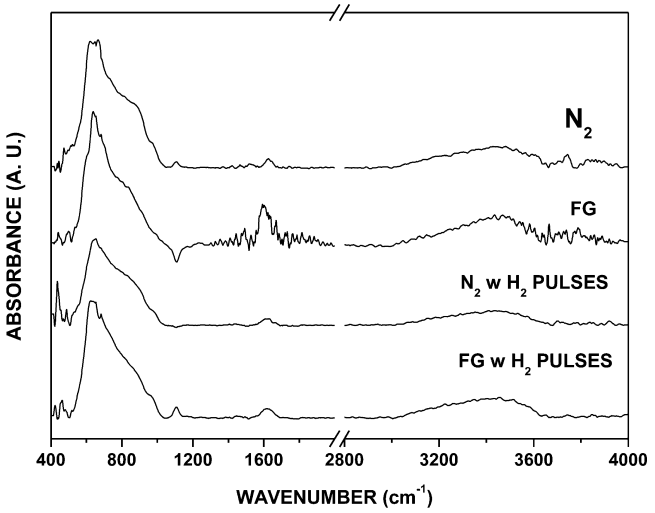

Figure 3. FTIR spectra taken on tungsten oxide samples grown in N_2 and FG environments without and with simultaneous pulsed injection of atomic hydrogen. The substantial differentiation of spectrum taken on the sample grown in FG relatively to the others can be observed.

with simultaneous pulsed exposure to atomic hydrogen. Typically, the FTIR spectra of tungsten oxide layers within the range 400−4000 cm^{-1} may be roughly divided in four regions:[38,39] 400−500 cm^{-1} where the vibration modes of the W−O bond are manifested, 500−1100 cm^{-1} related to the vibration of the W−O−W and O−W−O chains,[37,38] 1300−1800 cm^{-1} related to the vibrations of H−O−H and W−OH,[39] and 3000−3600 cm^{-1} where vibrations due to the presence of W−OH and of adsorbed H_2O appear.[40−42]

The spectrum of the sample grown in N_2, which as shown before is nearly stoichiometric, exhibits the above typical features with an additional shoulder near 910 cm^{-1} attributed to the W═O bond[37,38] and secondary peaks attributed to adsorbed water vapor. (See also Figure S3 in the Supporting Information.)

The most striking characteristic of the FTIR spectrum of the film grown in FG environment is the multiple peaks observed at the region near 1590 cm^{-1}, which, as previously mentioned, are related to vibrations of H−O−H chains and of W−OH.[39] The possibility of random effects (noise) was excluded because there was a one-by-one correspondence of peaks on the spectra of four samples deposited at different thicknesses. (See Figure S4 in the Supporting Information.) The existence of O−H bonds either in the form of water or of hydroxyl radicals is in agreement with the conclusions drawn from the XPS measurements previously presented. The presence of water in sample is also evidenced by the multiple peaks observed within the range 3200−3900 cm^{-1}. These multiple peaks were attributed in the past to the formation of hydrogen bonds between the OH groups in films.[24,37,43,44]

The FTIR spectra of the tungsten oxide samples grown in N_2 and FG environments and pulsed exposed to atomic hydrogen are completely smoothed-out relatively to the one in FG, as observed in Figure 3. (See also Figures S5 and S6 in the Supporting Information.) Moreover, peaks within the range 3200−3900 cm^{-1} related to adsorbed water and hydrogen bonds between OH groups also disappear from the spectra. This observation corroborates the conclusion drawn from the discussion of the XPS spectra (Figures 1 and 2) that the oxygen substoichiometry of these samples is due to the reaction of the atomic hydrogen with the OH^- radicals of the vapor, thus forming water molecules that escape in the deposition ambient under vacuum. A secondary plausible suggestion is that the remaining hydrogen in these samples, because it is not bonded to oxygen ions, is now bonded to the tungsten ions, as discussed further later. It is noted also that the water vapor adsorbed on samples shown in XPS measurements was not seen in the FTIR spectra probably because the former were made several days later, while the latter were made immediately after samples deposition.

It must be pointed out finally that in the previous discussion of FTIR spectra the peak near 1100 cm^{-1} was not assessed, although it is known to correspond to the vibration of W−OH bonds[45] because the silicon substrate also exhibits a strong peak at this wavelength.

f4 In Figure 4a is shown the energy dispersion of the real part, ε_1, of the dielectric constant, and in Figure 4b are shown the Tauc plots of various tungsten oxide samples grown in N_2 and FG environments without and with pulsed injection of hydrogen. It is observed that for the stoichiometric sample (grown in N_2) the dispersion of ε_1 is typical for an amorphous semiconductor and exhibits a band gap of 3.45 eV, in agreement with reported values for amorphous films.[6] The relatively low values of ε_1 are due to sample porosity.[22,24] The dispersion of ε_1 for the hydrogenated sample grown in FG is still typical of an insulator, but it exhibits oscillations due to additional absorption below the absorption threshold, also seen in Figure 4b, where two local maxima are observed near 2.9 to 3.0 and another near 1.0 eV, that is, approximately 0.6 to 0.8 and 2.2 to 2.5 eV, respectively, below the edge of the CB. For the sample grown in N_2 environment and exposed to atomic hydrogen, the ε_1 is shifted toward slightly higher values, and the band gap is now shifted to 3.9 eV due to a blue shift of the entire absorption edge probably related to the presence of hydrogen in the lattice. The two samples grown in FG with hydrogen injection stand apart; ε_1 exhibits regions where it takes negative values, while they still exhibit a band gap, which is typical of degenerate semiconductor.[7] This indicates that the exposure of these hydrogenated samples to atomic hydrogen has created delocalized states at the bottom of the CB, so electrons excited there now oscillate freely. By increasing the number of pulses, that is, the hydrogen doping, the plasma frequency is blue-shifted, indicating the corresponding increase in the number of free electrons. The sample grown with five hydrogen pulses during growth also exhibits a gap of 3.45 eV, similarly to the samples in N_2 and FG, which is probably a coincidence because the slope of the absorption edge decreases now significantly, indicating a significant alteration of the edge of the VB. A higher number of hydrogen pulses causes a further reduction of the tungsten oxide samples, and the gap shifts toward 2.5 eV, indicating that not only does the number of free

dx.doi.org/10.1021/jp502092h | J. Phys. Chem. C XXXX, XXX, XXX−XXX

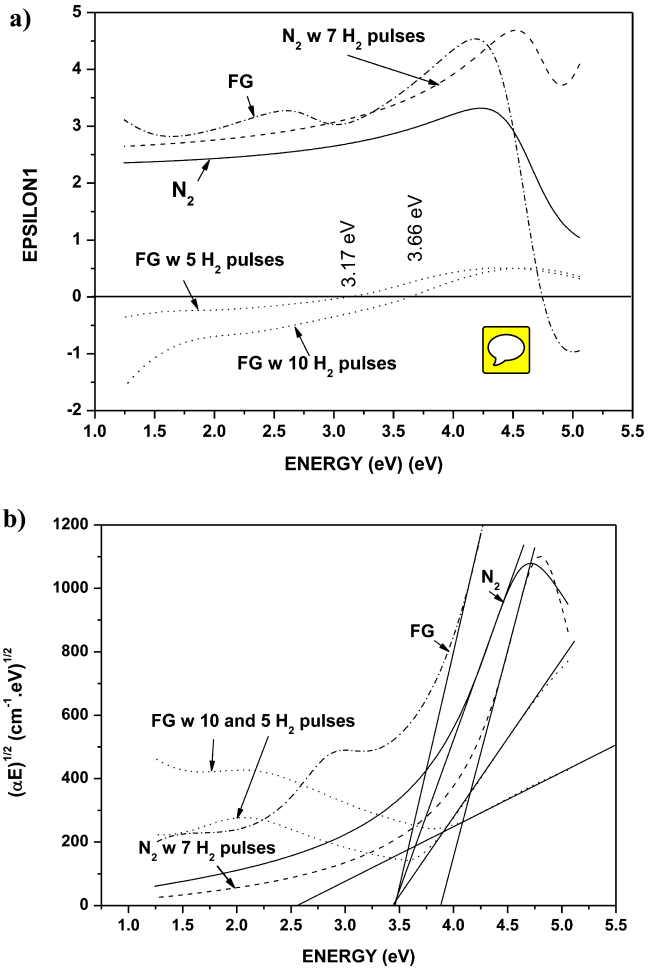

Figure 4. (a) Photon energy variation of the real part of dielectric constant, ε_1, for tungsten oxide samples grown in N_2, FG, environments without and with simultaneous pulsed injection of H_2. For the last samples, a plasma frequency is observed at 3.17 eV, which is shifted to 3.66 eV as the number of H_2 pulses increases. (b) Tauc's plots for tungsten oxide samples grown as in panel a. It is observed that all films exhibit a band gap, which starts to decrease at high exposures to atomic hydrogen (10 H_2 pulses).

electrons increase but also the whole electronic structure of samples starts to be perturbed considerably. Another point that must be noted is that the free electrons at the bottom of the CB are mainly supplied by the hydrogen. Because then the bottom of the CB is formed by tungsten 5d orbitals, these free electrons are now shared between the hydrogen 1s and the last. This indicates that now the hydrogen ions (or at least some of them) are incorporated into the lattice by bonding with the tungsten ions as opposed to samples grown in FG environment, where the last was incorporated by bonding with the oxygen ions, as previously seen. The presence of such W−H bonds is expected to alter the original electronic structure and is compatible with the significant changes of the slopes of the corresponding absorption edges of all samples deposited with pulsed hydrogen injection observed in Figure 4b.

To give a "geometrical" perception of the bonding of hydrogen with tungsten ions, we must note that the exponential factor of the 5d orbitals has the form $e^{-r/n}$, where r is the distance from the ion and n = 5 (the principal quantum number). This means that the 5d orbitals, despite their directional character, practically extend over the entire space surrounding the WO_6 octahedra. Moreover, the disordered nature of our samples reinforces the complete coverage of the space around the octahedra by 5d orbitals. A W−H bond may be formed either between ions located at neighboring lattice sites (the hydrogen replacing a vacant oxygen) or between a W ion at the center of an octahedron and a hydrogen ion located (randomly) at every possible position around it. Because of the narrowness of the d bands, bonds involving 5d electrons are expected to be relatively weak. The extended character of bonds involving 5d orbitals combined with their weakness is probably related to the chromic, the catalytic, and the (reversible) gas-sensing properties of tungsten oxide. Contrary to the above, the 4d Mo electrons are more localized near the parent ion and more directional, and this causes essential differences between the oxides of W and of Mo. In the last, as seen previously,[29] the inserted hydrogens are localized between O ions and, at high concentrations, between the double layers formed in this material, that is, in both cases near the Mo ion and at specific directions relative to it.

Figure 5 shows the low BE region of the UPS spectra of the tungsten oxide films. In the curve corresponding to the

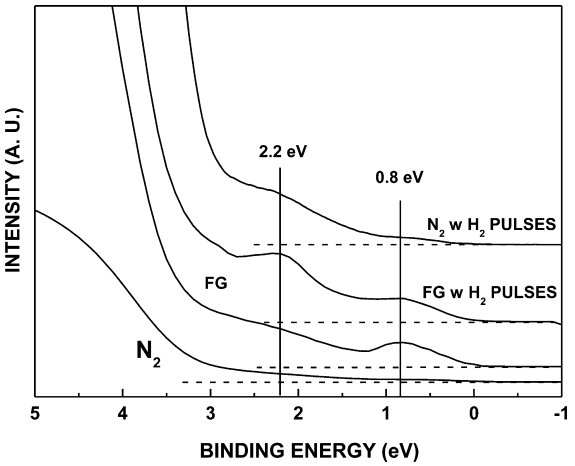

Figure 5. UPS spectra of the amorphous tungsten oxides in this study. The presence of oxygen vacancies (substoichiometry) causes the appearance of electronic states at 2.2 eV while the incorporated hydrogen is at 0.8 eV. The Fermi level was taken as zero.

stoichiometric tungsten oxide sample (deposited in N_2), the top of the VB maximum is located at 3.0 ± 0.1 eV below the Fermi level, and because the band gap is 3.45 eV, the material is negatively (n) doped. This is due to the slight oxygen substoichiometry of the sample imposed by thermodynamics and in view of the huge difference between the atomic weights of tungsten and oxygen. It can be observed that the states related to oxygen defects appear just above the top of the VB and spread in the band gap decreasing with energy, in agreement with previous works.[8,13,19]

The spectrum of film deposited in FG exhibits a large density of occupied gap states (forming IBs) exhibiting two local maxima at approximately 2.2 and 0.8 eV below the Fermi level, while the top of the VB remains nearly at the same energy as for the case of the stoichiometric film. In view of the positioning of the gap states related to oxygen defects deep within the gap seen before, it is reasonable to suggest that the maximum at 2.2 eV is related to oxygen vacancies, while the one at 0.8 eV is related to the inserted Hydrogen ions. Electronic transitions between these IBs and the CB justify the

dx.doi.org/10.1021/jp502092h | J. Phys. Chem. C XXXX, XXX, XXX−XXX

sub-band-gap absorption observed in Figure 4b. (See also Figure S7 in the Supporting Information, where the energy distribution of the joint density of states near the band gap is qualitatively depicted.) The sample grown in N_2 and exposed to atomic hydrogen is oxygen-deficient and contains small amounts of hydrogen, as seen before, so the shallower IB at 0.8 eV is remarkably attenuated relatively to the deeper one at 2.2 eV. In the UPS spectrum of sample deposited in FG with H_2 pulsed injection, it is observed that except for the IB at 2.2 eV, the one near the Fermi level is particularly strong and spreads toward higher energies, so electrons may be excited thermally to the bottom of the CB, giving the plasma absorption shown in Figure 4. The existence of an IB within the band gap of WO_3 has been reported in the past for materials doped with various methods such as ionic insertion, electron irradiation, and electro- and photocoloration.[8,12,13,18−20] However, the existence of two separate IBs, a deeper one related to oxygen defects and another closer to the Fermi level related to the dopants, to our knowledge, has not been reported.

In Figure 6 are shown the PL spectra for tungsten oxide films grown in N_2 and FG environments without and with H_2 pulsed injection. It can be observed that the (nearly) stoichiometric sample (grown in N_2) exhibits a sharp peak at 3.7 eV, very near the excitation energy (3.81 eV), indicating that practically no relaxation of the photoexcited electrons occurs during the process. The peak exhibits a full width at half-maximum of 0.03 eV, so a simple calculation presented before for amorphous molybdenum oxide films[29] based on the uncertainty principle can be made to show that this peak is due to the decay of excitons formed in the amorphous regions of the film rather than at the crystalline ones, which have dimensions of 3−5 nm only. (See Figure S1 in the Supporting Information). A secondary PL peak is also observed near 3.6 eV and some weak emission within the range 3.0 to 3.5 eV. There exist a rather extended literature on PL emission of WO_3 referring to crystalline samples, nanostructured in various forms.[46−53] Although the exact composition and the structure and the microstructure of samples are expected to influence the exact positioning of the PL peaks due to quantum confinement effects,[50] the peaks at 3.7 and 3.6 eV have been observed before,[47,48] while doublets of peaks distant by 0.1 to 0.2 eV have been reported at energies between 3.4 and 3.2 eV.[49−53]

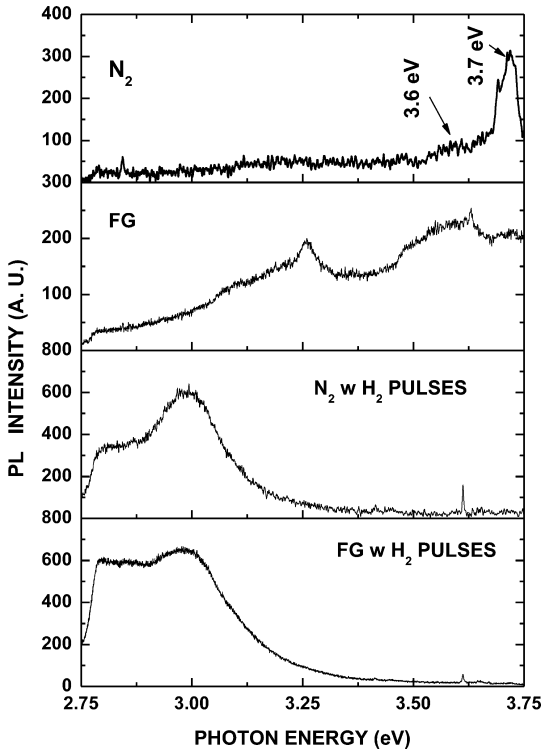

Figure 6. Photoluminescence spectra taken with excitation radiation of 3.81 eV on three tungsten oxide samples grown in N_2 and FG environments without and with simultaneous pulsed injection of H_2.

As seen before, the sample grown in FG contains OH^- ions connected between them with hydrogen bonds and exhibits IBs within the gap. Its PL spectrum shows similarities with others found in literature related to tungsten oxide samples grown from aquatic solutions, which most probably also contain such species,[47,48,52] and to the spectrum of a sample composed of $WO_3 \cdot H_2O$.[54] Also, the PL spectrum is very similar to that of hydrogen containing molybdenum oxide;[29] therefore, similar to this material, it may be understood considering electronic transitions between the d bands of the CB and the IBs within the band gap, which are also of d nature, as discussed next.

For tungsten oxide samples exposed to atomic hydrogen the PL spectrum are rel[illegible]fted, while the emission above 3.1 to 3.2 eV is completely quenched independent of the hydrogen doping of samples. This can be attributed to the presence of W−H bonds seen before in these samples, forming a CB whose bottom is composed not only of the 5d tungsten orbitals but also of the hydrogen 1s, thus forming extended wave functions. It is noted here that d bands are, in general, narrow; therefore, the corresponding wave functions even for crystalline materials are considered to be localized.[55] It seems then that the mixing of these d orbitals with the 1s of hydrogen leads to the formation of extended wave functions. A reasonable suggestion that can be made to explain the quenching of PL transitions at high energies is that due to the much higher ionization potential of hydrogen compared with that of tungsten, the free electrons at the bottom of the CB remain closer to the hydrogen ions, far away, as seen before from the holes formed at the W ions, so their recombination is now forbidden. The PL spectra are further discussed later in connection to the proposed electronic structure of amorphous tungsten oxide.

The main results reported so far are summarized in Table 1. It is seen that the (nearly) stoichiometric sample grown in

Table 1. Summary of Results Obtained from XPS, UPS, FTIR, and SE Measurements

sample	W^{+5} (%)	OH (%)	W−OH H−O−H	oxygen vacancies	states 0.8 eV below FL	states 2.2 eV Below FL	edges of VB and CB
N_2	0	0	adsorbed water	few	none	few	O 2p-W 5d
FG	20	26	many	few	many	few	O 2p-W 5d
N_2 + H_2 pulses	7	9.5	no	many	none-few	many	also contribution of H 1s
FG + H_2 pulses	25	16.5	no	many	many	many	also contribution of H 1s

dx.doi.org/10.1021/jp502092h | J. Phys. Chem. C XXXX, XXX, XXX−XXX

N_2,does not exhibit W^{5+} ions and OH^- radicals. As shown at the discussion of the FTIR spectra, there exist some hydrogen-bonded O−H−O bridges due to water molecules absorbed from the ambient air and some oxygen vacancies expected from thermodynamics. Because of the existence of these vacancies, states appear deeply within band gap extended at energies between 2 and 3 eV below the Fermi level, as shown before (Figure 5). A schematic representation of the energy variation of the DOS in sample is depicted in Figure 7a based on a model proposed for ReO_3[56] and more recent band structure calculations.[21,57,58] It is seen that the top of the VB is formed by the O 2p orbitals, while the W 5d orbitals are shifted ∼0.5 eV below. The bottom of the CB is composed of W 5d* (d_{xz}) and O 2p* antibonding orbitals, with the former having a larger contribution than the latter. The top of the CB is composed mainly of W 4d* (d_z^2) and to a lesser degree by O 2p* antibonding orbitals. Electronic states within the band gap are seen above the top of the VB, which are also of d character.[21,59] The optical absorption is due to electronic transitions between the valence and CBs, while the PL emission at 3.7 eV is due to transitions between the W 5d antibonding states at the bottom of the CB and the bonding ones at the top of the VB. Correspondingly, the PL peak at 3.6 eV may be attributed to transitions between the 5d* and the d states within the band gap. This means that the PL emission (Figure 6) is due to the decay of excitons formed on the W ions. In previous reports,[51,53] the PL emission in substoichiometric tungsten oxide was related to the presence of oxygen vacancies in samples. This conclusion is in agreement with the proposed electronic structure because oxygen vacancies are producing d states within the band gap.

For films grown in FG, the percentage of W^{5+} ions is lower (20%) than that of OH^- ions (26%). Considering that each OH^- corresponds to one W^{5+} ion while one oxygen vacancy corresponds to two such ions and that vacancies exist inherently into the tungsten−oxygen network, it is concluded that except for W−OH there exist excess (at least 6%) H ions in the network probably stabilized with O−H−O bridges connected between them with hydrogen bonds whose vibrations give the peaks near 1500 and within the range 3200−3800 cm^{-1} of the FTIR spectrum (Figure 3). A schematic of the energy variation of the DOS for this sample is shown in Figure 7b. Essentially VBs and CBs have similar composition as for the stoichiometric material with additionally the two IBs that are formed now. The fundamental absorption shown in Figure 4b is due to electronic transitions between VB and CB, while the PL emission is due to transitions between the various d-like antibonding states at the CB and the corresponding bonding ones at the VB and the IBs, as shown in Figure 7b.

For samples deposited in FG and exposed to atomic hydrogen, the number of W^{5+} ions is higher than that of OH^- radicals, indicating that now there exist a large number of oxygen vacancies into the network. This is shown on the UPS spectrum, which exhibits a strong peak at 2.2 eV (Figure 5). The lack of vibrations corresponding to hydrogen bonds from the FTIR spectrum indicates that the hydrogen ions are now stabilized within the network in a different way than for samples grown in FG (forming O−H−O bridges). The scenario presented before, based on the large extent of the W 5d orbitals, also explains the delocalization of the electronic wave functions seen in the discussion of Figure 4 manifested as plasma oscillation, which is unusual in amorphous metal-oxides

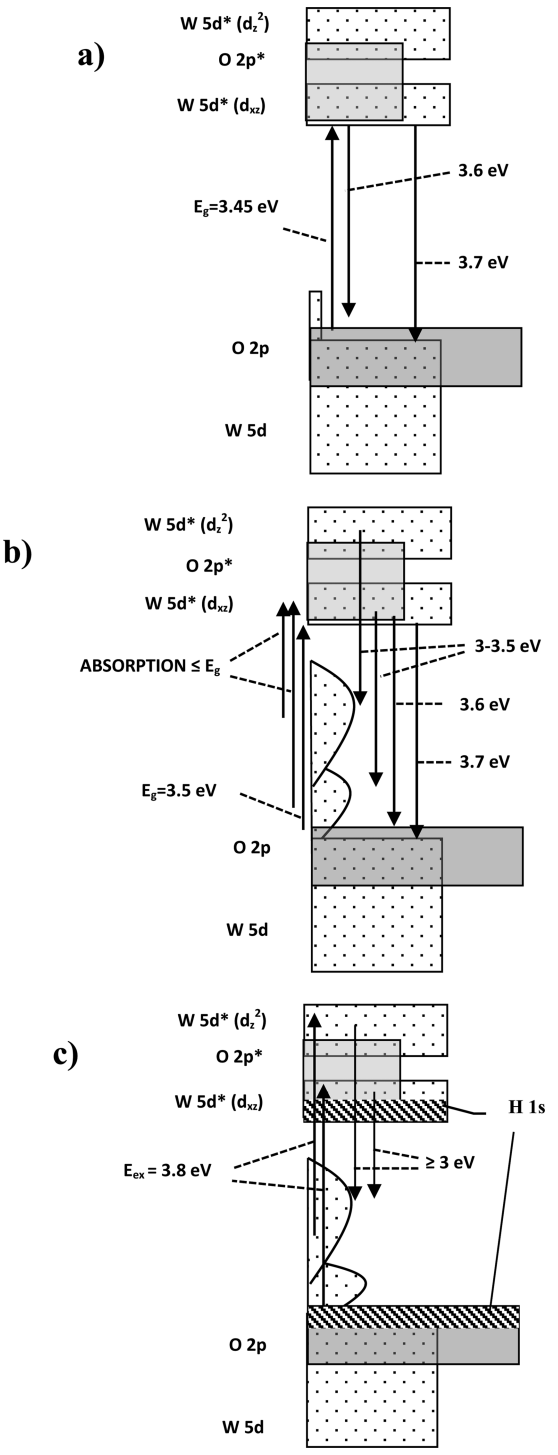

Figure 7. Schematic representation of the band structure of tungsten oxide films grown in N_2 (a) and in FG (b) environments and in N_2 and FG environments with hydrogen pulsed injection (c). The appearance and evolution of IBs within the band gap, caused by oxygen substoichiometry and hydrogen in lattice, are observed. The top and bottom of the valence and conduction band, respectively, in panel c are formed with the contribution of hydrogen 1s orbitals that create extended electronic states, which quench the corresponding PL transitions. The density of states is represented on the horizontal axis (not in scale) and the energy on the vertical. Arrows pointing upward correspond to optical absorption (Figure 4b), while those pointing downward correspond to PL emission (Figure 6) electronic transitions.

dx.doi.org/10.1021/jp502092h | J. Phys. Chem. C XXXX, XXX, XXX−XXX

with unfilled, narrow, d bands.[55] The presence of W−H bonds finally is in agreement with the significant distortion of the electronic structure of the amorphous tungsten oxide shown as gap narrowing in atomic hydrogen-exposed samples in Figure 4b.

The proposed schematic of the energy variation of the DOS for this sample is shown in Figure 7c. Valence and conduction bands have similar composition as that for the stoichiometric material, and there exist two IBs, a deeper one due to oxygen vacancies and another due to the presence of hydrogen in the network as for the material deposited in FG. Because the hydrogen ions share electrons with the W 5d orbitals, VBs and CBs now contain contributions from the H 1s orbitals, which above a certain limit start to distort the whole band structure considerably. (See Figure 4b.) The bottom of the CB is now composed of extended states, and this justifies the plasma oscillations seen before. Also, the excited electrons during the PL excitation do not remain near the corresponding holes but are free to move away, so the PL emission due to transitions between electrons at the bottom of the CB and holes at the VB and the IBs is now quenched. On the contrary, PL emission is observed at lower energies, corresponding to transitions between the d_z^2 electrons and the IBs, as seen in Figure 7c.

The case of the sample grown in N_2 and exposed to atomic hydrogen pulses is similar to that previously discussed. The energy variation of the DOS is again as in Figure 7c with the magnitude and the width of the "shallow" IB (corresponding to hydrogen) smaller this time, as seen at the UPS spectrum and justified by the small amount of hydrogen in the network. (See Table 1.) Although the bottom of the CB is composed of extended states, thus shifting PL emission toward lower energies, as in the previous case, no plasma oscillations are observed due to the presence of a few donor atoms (hydrogen ions) in the network. The high magnitude of the band gap in this case is possibly due to the passivation of states within the gap and the delocalization of wave functions near the edges of VB and CB by the hydrogen ions, as in the case of amorphous silicon, where hydrogenation implies a significant gap broadening relatively to the unhydrogenated material.[60]

IV. SUMMARY AND CONCLUSIONS

In this work, the influence of the oxygen substoichiometry and of the hydrogen incorporation on the electronic band structure of amorphous tungsten oxide films was studied. Because of the remarkable rigidity of the W−O network, which remains intact upon insertion/extraction of light ions, it was believed that the corresponding electronic structure is equally robust to the previously described factors, which were considered to cause only small alterations such as IVCT on a background similar to the pristine material or interband electronic oscillations. Here we have shown that contrary to the previous suggestion the electronic structure of the amorphous tungsten oxide is very sensitive to those factors. The oxygen substoichiometry (inherent or induced) causes the appearance of a band within the band gap ∼3 eV, while the incorporation of hydrogen causes another ∼1 eV below the edge of the CB. Both IBs are optically active and significantly influence the optical properties of the material. The hydrogen is incorporated into the W−O network either by bonding with the oxygen, thus forming O−H−O bridges, or, when the material is exposed to atomic hydrogen, directly bonded to the W ions sharing electrons with their 5d orbitals. Because of the extended character of the last, the presence of the two ions at adjacent lattice sites to form a W−H bond is not necessary, but the hydrogen may be located randomly around the WO_6 octahedron. If the hydrogen is incorporated into the lattice by forming O−H−O bridges, the electronic structure of the material has the characteristics of an amorphous metal-oxide semiconductor with unfilled d levels, exhibiting a band gap, localized wave functions at the edges of valence and conduction bands, and, additionally, two IBs. If W−H bonds are formed, the 1s orbitals of the hydrogen also participate in the formation of the top of VB and the bottom of the CB and cause the delocalization of the corresponding wave functions. With further incorporation of hydrogen into the lattice, the material is doped at high levels, and its electronic structure exhibits, in addition to the IBs, characteristics of degenerated semiconductors such as plasma oscillations. The previous conclusions are valuable for applications based on amorphous tungsten oxide such as in catalysis, EC and gaschromic windows, gas sensors, and the modification of electrodes in hybrid organic−inorganic semiconductor devices.

■ ASSOCIATED CONTENT

Supporting Information

Bright-field and the corresponding dark-field TEM micrographs taken on a tungsten oxide sample grown in N_2 environments. Bright-field and dark-field TEM images taken on a tungsten oxide sample grown in FG environment. FTIR spectra taken on tungsten oxide films grown at different times in N_2 environment. FTIR spectra taken on tungsten oxide films grown at different times in FG environment. FTIR spectra taken on tungsten oxide films grown in FG environment at similar deposition times with simultaneous pulsed injection of H_2. FTIR spectra taken on tungsten oxide films grown in N_2 environment at similar deposition times (5 min) with simultaneous pulsed injection of H_2. Photon energy variation of the imaginary part of dielectric constant, ε_2, for tungsten oxide samples grown in: N_2, FG environments, and in FG environment with simultaneous pulsed injection of H. This material is available free of charge via the Internet at http://pubs.acs.org.

■ AUTHOR INFORMATION

Corresponding Author

*E-mail: d.davazoglou@imel.demokritos.gr.

Author Contributions

The manuscript was written through contributions of all authors. All authors have given approval to the final version of the manuscript.

Notes

The authors declare no competing financial interest.

■ ACKNOWLEDGMENTS

G.P. acknowledges financial support by IKY Fellowships of Excellence for Postgraduate Studies in Greece-Siemens.

■ REFERENCES

(1) Loopstra, B. O.; Rietveld, H. M. Further Refinement of the Structure of WO_3. *Acta Crystallogr.* **1969**, *B25*, 1420−1421.
(2) Salje, E. The Orthorhombic Phase of WO_3. *Acta Crystallogr.* **1977**, *B 33*, 574−577.
(3) Granqvist, C. *Handbook of Inorganic Electrochromic Materials*; Elsevier: New York, 1995.
(4) Wittwer, V.; Datz, M.; Ell, J.; Georg, A.; Graf, W.; Walze, G. Gasochromic Windows. *Sol. Energy. Mater. Sol. Cells* **2004**, *84*, 305−314.

(5) Davazoglou, D.; Georgouleas, K. Low Pressure Chemically Vapor Deposited WO_3 Thin Films for Integrated Gas Sensor Applications. *J. Electrochem. Soc.* **1998**, *145*, 1346−1350.
(6) In the literature, there appears to be a large variation in the reported values for the band gap of WO_3. For amorphous films, the reported values of band gap vary between 3.2 and 3.5 eV. (a) Deb, S. K. Optical and Photoelectric Properties and Colour Centres in Thin Films of Tungsten Oxide. *Philos. Mag.* **1973**, *27*, 801−822. (b) Nakamura, A.; Samada, Y. Fundamental Absorption Edge of Evaporated Amorphous WO_3 Films. *Appl. Phys. A: Mater. Sci. Process.* **1981**, *24*, 55−59. For polycrystalline films, the gap values range within 2.6 and 2.9 eV. (c) Berak, J. M.; Sienko, M. J. Effect of Oxygen-Deficiency on Electrical Transport Properties of Tungsten Trioxide Crystals. *J. Solid State Chem.* **1970**, *2*, 109−133. (d) Hardee, K. L.; Bard, A. J. Semiconductor Electrodes: X. Photoelectrochemical Behavior of Several Polycrystalline Metal Oxide Electrodes in Aqueous Solutions. *J. Electrochem. Soc.* **1977**, *124*, 215−224. (e) Davazoglou, D.; Leveque, G.; Donnadieu, A. Study on the Optical and Electrochromic Properties of Polycrystalline WO_3 Thin Films Prepared by CVD. *Sol. En. Mater.* **1988**, *17*, 379−390. The film stoichiometry and density also influence the band gap in nanocrystalline films, where values between 2.8 and 3.2 eV are reported. (f) Vemuri, R. S.; Engelhard, M. H.; Ramana, C. V. Correlation between Surface Chemistry, Density, and Band Gap in Nanocrystalline WO_3 Thin Films. *ACS Appl. Mater. Interfac.* **2012**, *4*, 1371−1377.
(7) Owen, J. F.; Teegarden, K. J.; Shanks, H. R. Optical Properties of the Sodium-Tungsten Bronzes and Tungsten Trioxide. *Phys. Rev. B* **1978**, *18*, 3827−3837.
(8) Brigans, R.; Hochst, H.; Shanks, H. Defect States in WO_3 Studied with Photoelectron Spectroscopy. *Phys. Rev. B* **1981**, *24*, 3481−3489.
(9) Faughnan, B. W.; Crandall, R. S.; Heyman, P. M. Electrochromism in WO_3 Amorphous Films. *RCA Rev.* **1975**, *36*, 177−197.
(10) Chazalviel, J. N.; Campagna, M.; Wertheim, G.; Shanks, H. Final-State Effects in the X-Ray Photoelectron Spectra of Cubic Sodium-Tungsten Bronzes. *Phys. Rev. B* **1977**, *16*, 697−705.
(11) Schirmer, O. F.; Wittwer, V.; Baur, G.; Brand, G. Dependence of WO_3 Electrochromic Absorption on Crystallinity. *J. Electrochem. Soc.* **1977**, *124*, 749−753.
(12) Criticizing naively the IVCT model, it is noted that it foresees an initial increase in coloration with doping, as the population of W^{5+} ions increases at the expense of that of W^{6+}, up to a maximum when the two populations are equal, while a further increase in the doping (and correspondingly of the population of W^{5+} at the expense of W^{6+}) should have to lead to the complete bleaching when the valence of all tungsten ions turns to +5.
(13) (a) Hochst, H.; Brigans, R.; Shanks, H.; Steiner, P. Failure of the Rigid Band Model in Na_xWO_3: An XPS study. *Solid State Commun.* **1980**, *37*, 41−44. (b) Hochst, H.; Brigans, R.; Shanks, H. Electronic Structure of Na_xWO_3: A Photoemission Study Covering the Entire Concentration Range. *Phys. Rev. B* **1982**, *26*, 1702−1712.
(14) Lightsay, P.; Lilienfeld, D.; Holcomb, D. Transport Properties of Cubic Na_xWO_3 near the Insulator-Metal Transition. *Phys. Rev. B* **1976**, *14*, 4730−4732.
(15) Mott, N. F. The Degenerate Electron Gas in Tungsten Bronzes and Highly Doped Silicon. *Philos. Mag.* **1977**, *35*, 111−128.
(16) Crandall, R.; Faughnan, B. Electronic Transport in Amorphous H_xWO_3. *Phys. Rev. Lett.* **1977**, *39*, 232−235.
(17) Deb, S. K. Opportunities and Challenges in Science and Technology of WO_3 for Electrochromic and Related Applications. *Sol. Energy Mater. Sol. Cells* **2008**, *92*, 245−258.
(18) Colton, R.; Guzman, A.; Rabalais, J. Electrochromism in Some Thin Film Transition Metal Oxides Characterized by X-Ray Electron Spectroscopy. *J. Appl. Phys.* **1978**, *49*, 409−416.
(19) Hollinger, G.; Duc, T. M.; Deneuville, A. Charge Transfer in Amorphous Colored WO_3 Films Observed by X-Ray Photoelectron Spectroscopy. *Phys. Rev. Lett.* **1976**, *37*, 1564−1567.
(20) Wertheim, G.; Campagna, M.; Chalzalviel, J.; Buchannan, D.; Shanks, H. Electronic Structure of Tetragonal Tungsten Bronzes and Electrochromic Oxides. *Appl. Phys.* **1977**, *13*, 225−230.
(21) de Wijs, G. A.; de Groot, R. A. Structure and Electronic Properties of Amorphous WO_3. *Phys. Rev. B* **1999**, *60*, 16463−16474.
(22) Papadimitropoulos, G.; Vourdas, N.; Giannakopoulos, K.; Vasilopoulou, M.; Davazoglou, D. Porous Hot-Wire Deposited WO_3 Films with High Optical Transmission. *J. Appl. Phys.* **2011**, *109*, 103527−103533.
(23) Vourdas, N.; Papadimitropoulos, G.; Kostis, I.; Vasilopoulou, M.; Davazoglou, D. Substoichiometric Hot-Wire WO_x Films Deposited in Reducing Environment. *Thin Solid Films* **2012**, *520*, 3614−3619.
(24) Kostis, I.; Vourdas, N.; Vasilopoulou, M.; Douvas, A.; Papadimitropoulos, G.; Konofaos, N.; Iliadis, A.; Davazoglou, D. Formation of Stoichiometric, Sub-Stoichiometric Undoped and Hydrogen Doped Tungsten Oxide Films, Enabled by Pulsed Introduction of O_2 or H_2 during Hot-Wire Vapor Deposition. *Thin Solid Films* **2013**, *537*, 124−130.
(25) Vasilopoulou, M.; Palilis, L.; Georgiadou, D.; Douvas, A.; Argitis, P.; Kennou, S.; Sygellou, L.; Papadimitropoulos, G.; Kostis, I.; Stathopoulos, N.; Davazoglou, D. Reduction of Tungsten Oxide: A Path Towards Dual Functionality Utilization for Efficient Anode and Cathode Interfacial Layers in Organic Light-Emitting Diodes. *Adv. Funct. Mater.* **2011**, *21*, 1489−1497.
(26) Vasilopoulou, M.; Palilis, L.; Georgiadou, D.; Argitis, P.; Kennou, S.; Kostis, I.; Papadimitropoulos, G.; Stathopoulos, N.; Iliadis, A.; Konofaos, N.; Davazoglou, D.; Sygellou, L. Tungsten Oxides as Interfacial Layers for Improved Performance in Hybrid Optoelectronic Devices. *Thin Sol. Films* **2011**, *519*, 5748−5753.
(27) Vasilopoulou, M.; Papadimitropoulos, G.; Palilis, L. C.; Georgiadou, D. G.; Argitis, P.; Kennou, S.; Kostis, I.; Vourdas, N.; Stathopoulos, N. A.; Davazoglou, D. High Performance Organic Light Emitting Diodes Using Substoichiometric Tungsten Oxide as Efficient Hole Injection Layer. *Org. Electron.* **2012**, *13*, 796−806.
(28) Vasilopoulou, M.; Davazoglou, D. Hot-Wire Vapor Deposited Tungsten and Molybdenum Oxide Films Used for Carrier Injection/Transport in Organic Optoelectronic Devices. *Mater. Sci. Semicond. Process* **2013**, *16*, 1196−1216.
(29) Kostis, I.; Vourdas, N.; Papadimitropoulos, G.; Douvas, A.; Vasilopoulou, M.; Boukos, N.; Davazoglou, D. Effect of the Oxygen Sub-Stoichiometry and of Hydrogen Insertion on the Formation of Intermediate Bands Within the Gap of Disordered Molybdenum Oxide Films. *J. Phys. Chem. C* **2013**, *117*, 18013−18020.
(30) Sze, S. M. *VLSI Technology*; McGraw-Hill: New York, 1988.
(31) Barreca, D.; Carta, G.; Gasparotto, A.; Rossetto, G.; Tondello, E.; Zanella, P. A Study of Nanophase Tungsten Oxides Thin Films by XPS. *Surf. Sci. Spectra* **2001**, *8*, 258−267.
(32) Barreca, D.; Bozza, S.; Carta, G.; Rossetto, G.; Tondello, E.; Zanella, P. Structural and Morphological Analyses of Tungsten Oxide Nanophasic Thin Films Obtained by MOCVD. *Surf. Sci.* **2003**, *439*, 532−535.
(33) Weinhardt, L.; Blum, M.; Bar, M.; Heske, C.; Cole, B.; Marsen, B.; Miller, E. L. Electronic Surface Level Positions of WO_3 Thin Films for Photoelectrochemical Hydrogen Production. *J. Phys. Chem. C* **2008**, *112*, 3078−3082.
(34) Son, M. J.; Kim, S.; Kwon, S.; Kim, J. W. Interface Electronic Structures of Organic Light-Emitting Diodes with WO_3 Interlayer: A Study by Photoelectron Spectroscopy. *Org. Electron.* **2009**, *10*, 637.
(35) Höchst, H.; Bringans, R. D. Electronic Structure of Evaporated and Annealed Tungsten Oxide Films Studied with UPS. *Appl. Surf. Sci.* **1982**, *11/12*, 768−773.
(36) Wagner, C.; Davis, L.; Zeller, M.; Taylor, J.; Raymond, R.; Gale, L. Empirical Atomic Sensitivity Factors for Quantitative Analysis by Electron Spectroscopy for Chemical Analysis. *Surf. Interface Anal.* **1981**, *3*, 211−225.
(37) Dickens, G.; Crouch-Baker, S.; Weller, M. Hydrogen Insertion in Oxides. *Solid State Ionics* **1986**, *18&19*, 89−97.
(38) Daniel, F.; Desbat, B.; Lassegues, J. C.; Gerand, B.; Figlarz, M. Infrared and Raman Study of WO_3 Tungsten Trioxides and $WO_3{,}xH_2O$ Tungsten Trioxide Hydrates. *J. Solid State Chem.* **1987**, *67*, 235−247.

(39) Díaz-Reyes, J.; Dorantes-Garcia, V.; Pérez-Benítez, A.; Balderas-López, J. A. Obtaining of Films of Tungsten Trioxide (WO3) by Resistive Heating of a Tungsten Filament. *Superficies Vacio* **2008**, *21*, 12−17.
(40) Pfeifer, J.; Guifang, C.; Tekula-Buxbaum, P.; Kiss, B. A.; Farkas-Jahnke, M.; Vadasdi, K. A Reinvestigation of the Preparation of Tungsten Oxide Hydrate WO_3, $1/3H_2O$. *J. Solid State Chem.* **1995**, *119*, 90−97.
(41) Gotić, M.; Ivanda, M.; Popović, S.; Music, S. Synthesis of Tungsten Trioxide Hydrates and Their Structural Properties. *Mater. Sci. Eng.* **2000**, *B77*, 193−201.
(42) Yalamanchili, M.; Atia, A.; Miller, J. Analysis of Interfacial Water at a Hydrophilic Silicon Surface by In-Situ FTIR/Internal Reflection Spectroscopy. *Langmuir* **1996**, *12*, 4176−4184.
(43) The infrared spectrum of water exhibits a multitude of peaks within the region 1300−1600 cm^{-1} due to the so-called librations of its molecule. A very good review can be found at the address: http://www.lsbu.ac.uk/water/vibrat.html.
(44) Kostis, I.; Vasilopoulou, M.; Papadimitropoulos, G.; Stathopoulos, N.; Savaidis, S.; Davazoglou, D. Deposition of Undoped and H Doped WO_x ($x \leq 3$) Films in a Hot-Wire Atomic Layer Deposition System Without the Use of Tungsten Precursors. *Surf. Coat. Technol.* **2013**, *230*, 51−58.
(45) Wright, C. J. Inelastic Neutron Scattering Spectra of the Hydrogen Tungsten Bronze $H_{0.4}WO_3$. *J. Solid State Chem.* **1977**, *20*, 89−92.
(46) Diaz-Reyes, J.; Flores-Mena, J. E.; Gutierrez-Arias, J. M.; Morin-Castillo, M. M.; Azucena-Coyotecatl, H.; Galván, M.; Rodríguez-Fragoso, P.; Mendez-López, A. *Advances in Sensors, Signals and Materials - 3rd WSEAS International Conference on Sensors and Signals*, SENSIG'10, 3rd WSEAS International Conference on Materials Science, MATERIALS'10; WSEAS Press: Greece, 2010; pp 99−104.
(47) Rajagopal, S.; Nataraj, D.; Mangalaraj, D.; Djaoued, Y.; Robichaud, J.; Khyzhun, O. Yu. Controlled Growth of WO_3 Nanostructures with Three Different Morphologies and Their Structural, Optical, and Photodecomposition Studies. *Nanoscale Res. Lett.* **2009**, *4*, 1335−1342.
(48) Wang, J.; Lee, P.; Ma, J. Synthesis, Growth Mechanism and Room-Temperature Blue Luminescence Emission of Uniform WO_3 Nanosheets with W as Starting Material. *J. Cryst. Growth* **2009**, *311*, 316−319.
(49) Lu, X.; Liu, X.; Zhang, W.; Wanga, C.; Wei, Y. Large-Scale Synthesis of Tungsten Oxide Nanofibers by Electrospinning. *J. Colloid Interface Sci.* **2006**, *298*, 996−999.
(50) Feng, M.; Pan, A. L.; Zhang, H. R.; Li, Z. A.; Liu, F.; Liu, H. W.; Shi, D. X.; Zou, B. S.; Gao, H. J. Strong Photoluminescence of Nanostructured Crystalline Tungsten Oxide Thin Films. *Appl. Phys. Lett.* **2005**, *86*, 141901−141903.
(51) Luo, J. Y.; Zhao, F. L.; Gong, L.; Chen, H. J.; Zhou, J.; Li, Z. L.; Deng, S. Z.; Xu, N. S. Ultraviolet-Visible Emission from Three-Dimensional WO_{3-x} Nanowire Networks. *Appl. Phys. Lett.* **2007**, *91*, 093124-1−093124-3.
(52) Lee, K.; Seo, W. S.; Park, J. T. Synthesis and Optical Properties of Colloidal Tungsten Oxide Nanorods. *J. Am. Chem. Soc.* **2003**, *125*, 3408−3409.
(53) Park, S.; Kim, H.; Jin, C.; Lee, C. Intense Ultraviolet Emission from Needle-Like WO_3 Nanostructures Synthesized by Noncatalytic Thermal Evaporation. *Nanoscale Res. Lett.* **2011**, *6*, 451.
(54) Niederberger, M.; Bartl, M. H.; Stucky, G. D. Benzyl Alcohol and Transition Metal Chlorides as a Versatile Reaction System for the Nonaqueous and Low-Temperature Synthesis of Crystalline Nano-Objects with Controlled Dimensionality. *J. Am. Chem. Soc.* **2002**, *124*, 13642−13643.
(55) Adler, D. Insulating and Metallic States in Transition Metal Oxides. In *Solid State Physics*; Academic Press: New York, 1968; Vol. *21*, pp 1−113.
(56) Goodenough, J. Narrow Band Electrons in Transition Metal Oxides. *Czech. J. Phys.* **1967**, *17*, 304−336.
(57) Bulett, D. Bulk and Surface Electron States in WO, and Tungsten Bronzes. *J. Phys. C* **1983**, *16*, 2197−2207.
(58) Stachiotti, M. G.; Cora, F.; Catlow, C. R. A.; Rodriguez, C. O. First-Principles Investigation of ReO_3 and Related Oxides. *Phys. Rev. B* **1997**, *55*, 7508−7514.
(59) Khyzhun, O.; Solonin, Y. Electronic Structure of Nanoparticles of Substoichometric Hexagonal Tungsten Oxides. *J. Phys. Conf. Ser.* **2007**, *61*, 534−539.
(60) Janai, M.; Allred, D.; Booth, D.; Seraphin, B. Optical Properties and Structure of Amorphous Silicon Films Prepared by CVD. *Sol. Energy Mater.* **1979**, *1*, 11−27.